DYNAMIC MODEL FOR UASB REACTOR INCLUDING REACTOR HYDRAULICS, REACTION, AND DIFFUSION

By May M. Wu[1] and Robert F. Hickey[2]

ABSTRACT: A dynamic model has been developed to describe upflow anaerobic sludge blanket (UASB) reactors from several aspects including reactor hydraulics, biological reaction kinetics, and mass transfer within anaerobic granules. A flow model of a nonideal continuously stirred tank reactor (CSTR) followed by a dispersion plug flow reactor (PFR) was used to simulate the reactor hydraulics as observed from a LiCl tracer study. The dynamic model based on this flow model was then evaluated by a set of acetate impulse data and verified with a data set from a two-step acetate feed increase experiment from a bench-scale UASB reactor. The model describes UASB reactor performance well. Simulation results indicate significant effects of reactor nonideal flow, diffusional resistance, as well as degradation kinetics on overall substrate utilization rate. Sensitivity analyses on model parameters K_s, k_m, K_L, D, R, and nonideal flow factors revealed granule size has a strong impact on the reactor performance. The effect of K_L is not significant. Reactor mixing was improved by an increase in biogas production.

INTRODUCTION

Considerable effort has been expended on developing a dynamic model for the anaerobic waste treatment process in order to optimize design and process control. Stoichiometric models were first established for a homogeneous system. Andrews (1969) presented a dynamic model describing a single culture (methanogens) substrate utilization, pH, bacterial growth (with inhibition by un-ionized acetic acid), alkalinity, and gas production. The interactions between gas, liquid, and biological phases within the anaerobic digester were considered (Andrews and Graef 1971). Similar approaches have been subsequently used to describe additional microbial populations and other parameters in modeling (Hill and Barth 1977; Carr and O'Donnell 1977; Mosey 1983; Rozzi et al. 1985). In the case of a fixed-film system, researchers have suggested that substrate utilization in biofilms may be limited by mass transfer resistance (Atkinson and Daoud 1970; Harremoës 1976; LaMotta 1976; Shieh et al. 1982; Kissel et al. 1984). Upflow anaerobic sludge blanket (UASB) reactors and fluidized bed reactors (FBR) are two of the biofilm processes developed that used immobilized biocatalyst. Bacterial granules in UASB are self-immobilized bioparticles whereas in FBRs, the biofilm is established on the media (supporting material), such as activated carbon. Growth and loss of steady-state biofilm and substrate flux was described by a biofilm model (Rittmann and McCarty 1980; Rittmann 1982). Methanogenic biofilm modeling for FBR and UASB has been concentrated on mass transfer limitations and single/multiple substrate aspects (Atkinson and How 1974; Atkinson and Davies 1974; Lin 1991; Alphenaar et al. 1993; Buffière and Steyer 1995; De Beer et al. 1992; Lens et al. 1993). A detailed analysis of mathematical modeling for fluidized bed bioreactors was provided by Andrews (1988). Many of these studies deal with steady-state conditions. Unsteady state is the most critical situation for modeling associated with real-time control strategies. Dynamic, diffusion-reaction biofilm models have been presented for aerobic processes considering both flat and spherical geometry for the biofilm (Benefield and Molz 1984). Bolte and Hill (1993) described attached growth anaerobic fermenters degrading a model animal waste using a reaction-diffusion dynamic model.

Because of the complexity of such processes, most dynamic models describe complete mixing flow (CMF) in the reactor. Mixing problems in UASB reactors have been a concern. An attempt was made to model UASB reactor using a flow model with sludge transport and kinetics (Bolle et al. 1985).

The primary goal of this study was to develop a dynamic model for UASB reactors with methanogenic anaerobic granules, on the basis of kinetics, mass transfer limitations, and integration of the reactor hydraulics. The reactor flow was modeled using tracer studies. The integrated dynamic model was evaluated using a data set when acetate impulse was applied to a bench-scale UASB reactor. Model verification was obtained using data from a two-step acetate loading rate increase experiment. Major factors that influenced reactor overall performance among kinetics, mass transfer, and reactor flow were identified. Different combinations of flow-kinetic-mass transfer models were compared. Sensitivity analysis was performed.

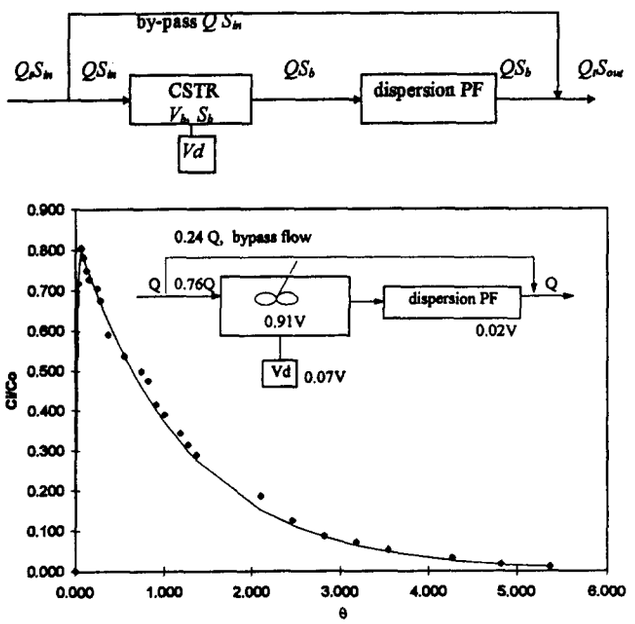

FIG. 1. UASB Reactor: (a) Representation of Hydraulic Model; (b) Results of Lithium Chloride Impulse Experiment and Simulated Response

[1]Post Doctoral Fellow, Waste Mgmt. and Bioengrg. Section, Energy Sys. Div., Argonne Nat. Lab., ES 362, 9700 S. Cass Ave., Argonne, IL 60439.

[2]Vice Pres., EFX Systems, Inc., 3900 Collins Rd., Ste. 1011, Lansing, MI 48910-8396.

Note. Associate Editor: Oliver J. Hao. Discussion open until August 1, 1997. To extend the closing date one month, a written request must be filed with the ASCE Manager of Journals. The manuscript for this paper was submitted for review and possible publication on October 25, 1995. This paper is part of the *Journal of Environmental Engineering*, Vol. 123, No. 3, March, 1997. ©ASCE, ISSN 0733-9372/97/0003-0244–0252/$4.00 + $.50 per page. Paper No. 11890.

MODEL DEVELOPMENT AND SOLUTION TECHNIQUE

UASB Flow Model

A flow model was first developed to describe UASB reactor hydraulics [Fig. 1(a)]. The sludge bed and blanket are represented by a nonideal continuously stirred tank reactor (CSTR) with dead volume and bypass flow. This CSTR is in series with a dispersion plug flow reactor (PFR) that represents the clarification zone above the sludge blanket. Equations of the flow model in the UASB are

$$V_b \frac{dC}{dt} = V_b E(t) - QfC(t) \tag{1}$$

$$E(t) = \begin{cases} \dfrac{Mf}{V_b T_{in}}, & \text{if } 0 \le t \le T_{in} \\ 0, & \text{if } T_{in} \le t \end{cases} \quad \text{for impulse} \tag{2}$$

where $C(t)$ = tracer concentration within CSTR; V_b = CSTR working volume; $E(t)$ = input function for tracer impulse; Qf = flow fraction that enters the working volume; Mf = fraction of mass input that go through reactor's working volume; and T_{in} = tracer injection time. Eq. (1) is a mass balance on the CSTR; while (2) describes a tracer input.

The equations for the dynamics of the tracer concentration C_{pf} in dispersion PFR are

$$\frac{\partial C_{pf}}{\partial t} = \frac{D_p}{L}\frac{\partial^2 C_{pf}}{\partial Z^2} - \frac{u}{L}\frac{\partial C_{pf}}{\partial Z}, \quad t > 0,\ 0 < Z < 1 \tag{3}$$

$$\text{BC: } C_{pf}(0, t) = C(t) \tag{4}$$

$$\text{IC: } C_{pf}(Z, 0) = C_o \tag{5}$$

where Z = vertical coordinate; D_p = dispersion coefficient; u = flow velocity within the PFR; and L = length of the PFR. A computer program written with FORTRAN has been developed to solve (1)–(5). The UASB dynamic model is then developed for the system by adding additional elements (substrate utilization, mass transfer, etc.) into the flow model.

UASB Reactor Dynamic Model

The UASB reactor dynamic model is comprised of three parts: substrate utilization within the biofilm (granules); mass transfer and transport in the granule bed and blanket; and mass transport within the clarifier (zone above the bed). Sludge bed in the UASB reactor is composed of anaerobic granules; the sludge blanket above the bed is a mixture of granules and flocs, with granules in majority. Substrate transport within granule bed and blanket is described by mass transfer into granule liquid film and advection. Due to high amount of biogas (CH_4 and CO_2) generated during methane fermentation, and that the dead volume and bypass flow exist in the bed, the bulk liquid in the bed and blanket is described by a nonideal CSTR. The liquid layer or clarification zone above the sludge blanket was slightly turbid. There are few granules and some flocs floating in the clarifier. Few flocs are at the liquid layer that attributes to some biological activity. However, the amount of biomass in the clarifier is much less compared to that in the granule bed and was neglected in modeling. The model describes the clarifier by advection and dispersion. Within each granule, coupled mass transfer and substrate utilization occur. Diffusional resistance can be minimized only under the condition that granules are present as flocs (μm range in diameter), observed from a study on these granules (Wu et al. 1995). Majority anaerobic methanogenic granules are around 3.0 mm in diameter (at the bottom half of the bed). These granules are comprised of five microbial populations: ethanol degrader, propionate utilizers, sulfate-reducing bacteria, methanogens grown on acetate, or hydrogen. Microscopy of granules shows that the majority of active cells [in this granule, *Methanobeata* (*Methanothrix*) is predominant] are concentrated in a 100 μm thick outer layer (Wu 1995), or the active layer. Cell density decreases dramatically at the central core where cells appeared in starvation. Empty space, inorganic deposits, and dead cells in the central core has been reported (Alphenaar et al. 1993). This unique structure is an indication of substrate deficiency in the center space. A granule model is established based on prior observations (Fig. 2), that shows the substrate (S_b) transporting from bulk liquid to a stagnant liquid film or boundary layer outside of the biofilm. A concentration gradient is established across the liquid film. Substrate then concurrently diffuses through the biofilm and is consumed (S_s). Substrate gradient is near zero on the inner surface of the outer biofilm layer. On the outer surface, in case of steady state, mass continuation hold at the interface of liquid layer and biofilm. However, at unsteady state, substrate accumulates at the interface. The accumulation might be transient and negligible, due to the fact that accumulation in substrate at the δ layer increases mass transfer into the central core where the substrate is consumed immediately because of some microbial activity. Several assumptions and simplifications are made for the proposed dynamic model: (1) granules are perfect spherical shells with a radius R of 1.5 mm; (2) substrate diffuses into granules, penetrating a layer with a thickness of δ from granule surface—at the inner edge of this layer, substrate gradient reaches zero; (3) degradation of acetate can be described by Monod kinetics; (4) acetate utilizers are evenly distributed throughout the entire active layer δ; (5) growth of acetate-utilizing methanogen is neglected due to its slow growth rate and relatively short period of the perturbation (i.e., 4 h) to the system; (6) mass continuity holds at the interfaces between bulk liquid and the liquid boundary layer, and between the liquid boundary layer and granule surface; (7) the granule bed can be described as a CSTR (substrate concentration in the liquid volume of the bed is uniform); (8) bypass flow and dead space are present within the reactor; (9) there is no substrate transporting into or out of the dead space; (10) substrate utilization in clarifier is negligible; and (11) the UASB reactor is operated at a steady state prior to impulse or step increase of acetate. By applying acetate mass balance on anaerobic granules, the granular bed, and the clarifier, respectively, the dynamic model equations are obtained as follows.

For anaerobic granules, we have

$$\frac{\partial S}{\partial t} = D\left(\frac{\partial^2 S}{\partial x^2} - \frac{2}{R - x}\frac{\partial S}{\partial x}\right) - \frac{k_m X_m S}{K_s + S} \tag{6}$$

$$\text{BCs: (i) } -D\frac{\partial S}{\partial x} + K_L S = K_L S_b, \quad x = 0 \tag{7}$$

$$\text{(ii) } \frac{\partial S}{\partial x} = 0, \quad x = \delta \tag{8}$$

$$\text{IC: (i) } S(x, 0) = S_s(x), \quad x \in (0, \delta) \tag{9}$$

where R = granule radius (mm); k_m = specific substrate utilization rate (g acetate/gVS-d); K_s = half velocity constant (mM); D = effective diffusion coefficient (m^2/s); K_L = mass transfer coefficient (mm/s); X_m = active acetate utilizer biomass density within the outer layer δ (gVS/cm^3); S = acetate concentration within biofilm (mM); S_b = bulk acetate concentration (mM); S_s = steady-state acetate concentration within biofilm (mM); finally, $x \in (0, \delta)$ is the spatial variable within the active layer where $x = 0$ represents the outer surface and $x = \delta$ the inner surface.

At the moment of impulse, substrate concentration within biofilm [$S(x, 0)$] is equal to that of steady-state concentration (S_s) (9), which is governed by the following equations:

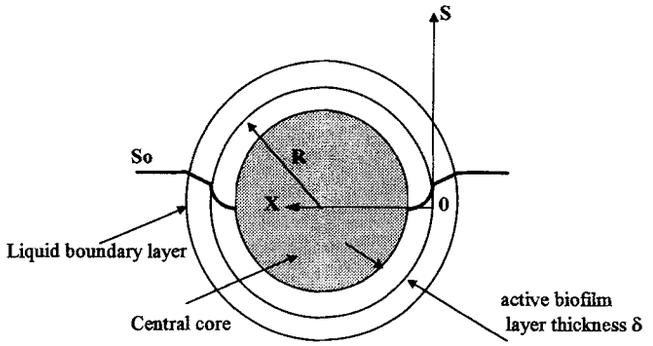

FIG. 2. Model for Brewery Granules with Central Core and Liquid Boundary Layer (R = Radius; S = Substrate Profile; S_o = Bulk Substrate Concentration)

$$D\left(\frac{\partial^2 S_s}{\partial x^2} - \frac{2}{R - x}\frac{\partial S_s}{\partial x}\right) = \frac{k_m X_m S_s}{K_s + S_s} \tag{10}$$

$$\text{BCs: (i)} \quad -D\frac{\partial S_s}{\partial x} + K_L S_s = K_L S_{bo}, \quad x = 0 \tag{11}$$

$$\text{(ii)} \quad \frac{\partial S_s}{\partial x} = 0, \quad x = \delta \tag{12}$$

where S_{bo} = steady-state acetate concentration in bulk liquid (mM/L). Immediately after the input, the reactor response is governed by (6)–(8). Mass balance on granule bed involves three terms: substrate input entering the reactor bed, leaving the bed, and transferring into granules and subsequently being utilized

$$V_b\frac{dS_b}{dt} = V_b E(t) - QfS_b(t) - K_L A_r[S_b - S(0, t)] \tag{13}$$

$$\text{IC: } S_b(0) = S_{bo} \tag{14}$$

$$E(t) = \begin{cases} \dfrac{Mf}{V_b T_{in}}, & \text{if } 0 \le t \le T_{in} \\ 0, & \text{if } T_{in} \le t \end{cases} \quad \text{for impulse} \tag{15}$$

$$E(t) = \begin{cases} QfS_{bkgd}, & \text{if } 0 < t < T_{stp1} \\ QfS_{stp1}, & \text{if } T_{stp1} \le t < T_{stp2} \\ QfS_{stp2}, & \text{if } T_{stp2} \le t \end{cases} \quad \text{for step increase} \tag{16}$$

where A_r = total granule surface area (mm^2); S_{bkgd} = influent substrate concentration before step increase (mM); S_{stp1} = influent substrate concentration at first step increase (mM); S_{stp2} = influent substrate concentration during the second step increase (mM); T_{stp1} = time when the first step is initiated (min); T_{stp2} = time that the second step is initiated (min); and T_{in} = substrate injection time for the acetate impulse (min). Other symbols are the same as that in (1)–(12). The last term in (13), $K_L A_r[S_b - S(0, t)]$, describes the substrate transferring from bulk solution through liquid boundary layer into the granules. Term $S(0, t)$ in (13) is the substrate concentration at liquid boundary layer-granule interface at time t, determined by (6) through (9). This term reflects the kinetic and diffusion process for the substrate (S_b) removal. There are two consecutive step increases in (16).

In the clarifier, the flow regime is represented by a dispersion PFR, as a result of bubbles raising from the bed through the liquid layer above the bed, biological reactions are ignored [assumption (10)]

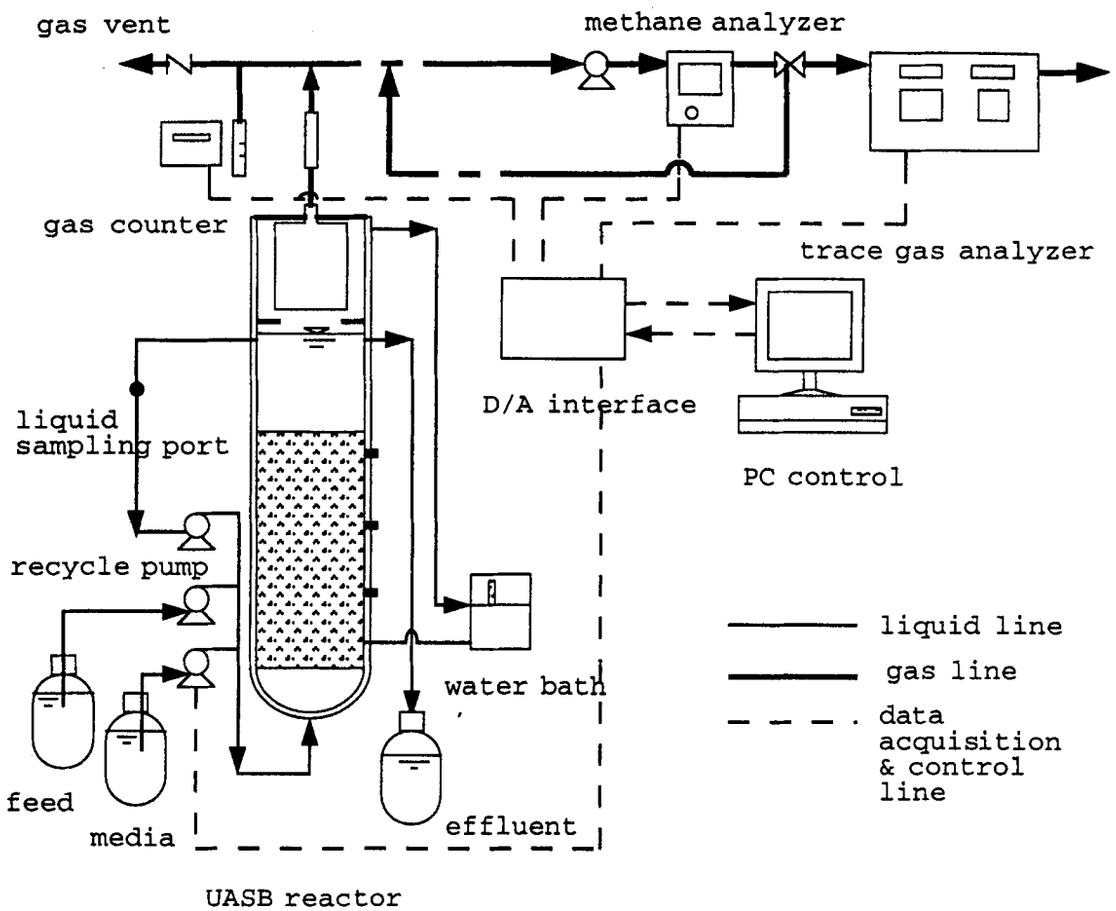

FIG. 3. Representation of Bench-Scale UASB Reactor with On-Line Data Acquisition System

TABLE 1. Experimental Conditions of Bench-Scale UASB Reactor during Acetate Impulse and Step OLR Increase Experiments

Parameter (1)	Value (2)
OLR (kgCOD/m³bed-d)	9–10
HRT (h)	11
Temperature (°C)	37
pH	6.8–7.1
Total flow rate (L/d)	6.6–6.7
Feed COD (kg/L)	11.4
Reactor total volume (L)	3.1
Reactor gas volume (L)	1.1
Bed volume (solids and liquid) (L)	1.6–1.7
Gas production rate (L/d)	5.3–6.7
Methane content (percent)	75–80

$$\frac{\partial S_d}{\partial t} = \frac{D_p}{L^2}\frac{\partial^2 S_d}{\partial Z^2} - \frac{u}{L}\frac{\partial S_d}{\partial Z}, \quad t > 0,\ 0 < Z < 1 \tag{17}$$

$$\text{BC: } S_d(0, t) = S_b(t) \tag{18}$$

$$\text{IC: } S_d(Z, 0) = S_{bo} \tag{19}$$

where S_d = substrate concentration in clarification zone (mM). Other symbols are the same as in (3)–(5) and (6)–(12).

The preceding equations are solved numerically, using a FORTRAN program. The ODEs are solved with international math subroutines library (IMSL) packages, and the PDE is solved with the finite-difference method (Ames 1977). Unit transformations are performed on the model equations, and are then scaled to simplify the computations.

MATERIAL AND METHODS

Bench-Scale UASB Reactor and Feed

The UASB reactor was all-glass, water-jacket, 50.4 mm (2 in.) diameter and 1.82 m (6 ft) tall, with a total volume of 3.1 L. The reactor system setup is presented in Fig. 3. Reactor mixing was provided through a recirculation pump. Liquid samples were taken from the sampling port at the recirculation line. The bench-scale UASB reactor was equipped with an on-line data acquisition and control system, PARAGON (Intec), through an analog/digital (A/D) interface (OPTO-22) and a personal computer (386). The UASB reactor has been operated at 37°C, pH = 7 (±0.2), an organic loading rate (OLR) range of 5–10 kgCOD/m³bed-d, and hydraulic retention time (HRT) of 0.5–2 d during acclimation period.

Anaerobic granules had been acclimated for more than six months to a synthetic brewery waste. Major components of this waste were ethanol (74 mM), propionate (25 mM), acetate (15 mM), and ferrous sulfate (0.6 mM as $SO_4^{=}$). The mineral components were presented elsewhere (Wu et al. 1995).

Modeling Experiments

Modeling experiments were conducted on the bench-scale UASB reactor treating a synthetic brewery waste. The bench-scale UASB was operated at OLR of 10 kgCOD/m³bed-d and HRT of 11 h. Presented in Table 1 are operational conditions of the modeling experiments. During tracer study, pulse input of lithium chloride solution (160 mg) was introduced through the UASB reactor recirculation line. Acetate of 52.7 mM was introduced into the system by pulse input during dynamic modeling experiment. The acetate step increase experiment was carried out by increase feed acetate concentration from 25 to 125 mM at the first step; and subsequently from 125 to 225 mM. The inlet flow rate was held constant. Other components of the synthetic brewery waste feed were not changed during the experiment. Gas production was monitored during each experiment. Steady state is assumed when reactor performance parameters varied no greater than 2% daily and the reactor has been operated at a hydraulic retention time of more than three.

Analytical Methods

Lithium chloride and sodium acetate (Sigma Chemical, reagent grade), were used as inert tracer and modeling substrate, respectively. For analysis of lithium, 5 mL samples were collected, filtered through a 0.2 μm syringe filter, and transferred into a 10 ml glass tube. For acetate measurement, samples were centrifuged (Brinkmann model 5415) at 12,000 rpm for 2 min. Supernatant was then collected and acidified (to 0.03 M oxalic acid).

Lithium concentration was determined by Flame Emission Spectroscopy (FES) (Spectra AA-20 Plus using air-acetylene). Analysis conditions were: wavelength 670.8 nm, slit width, 1.0 nm. A series dilution of five standards was made and triplicates were injected for calibration. Samples concentrations were calculated based on the standard curve. Check standards were injected with every batch of samples.

Acetate was analyzed using a HP 5890 GC equipped with a packed column and a Flame Ionization Detector (FID). Injection port temperature was 190°C, oven temperature was increased from 140 to 220°C (ramp 5°C/min), and the detector temperature was 220°C. Helium was the carrier gas at a flow rate of 16–18 mL/min. A standard curve was prepared for acetate and checked for linearity. Standards were injected with every batch of samples. Sample concentrations were determined based on the standard curve.

Parameter Estimation

Hydraulic model parameters V_b, f, D_p/L^2, and u/L were first estimated during tracer study. Following acetate impulse, hydraulic, mass transfer, and other reactor parameters were evaluated through model simulation. Kinetic parameters, k_m and K_s, were estimated through batch experiments (Wu et al. 1995). ε, R, δ, and Ar were measured from the UASB reactor bed and granules. Bed voidage, ε, was obtained by filtering a known volume bed sample and measuring the liquid volume. Granule radius, R, was estimated using an Olympus DF microscope. The same microscope was also used for observation of granule intrastructure and determine granule active (outer) layer thickness δ on a cross-section of granules. Granule surface area, A_r, was calculated from $A_r = V_{bed}(1 - \varepsilon)4\pi R^2/(4/3\pi R^2)$, X_m, K_L, D, D_p/L^2, u/L, V_b, and f were estimated by simulation. Presented in Table 2 are the dynamic model parameters, measured or simulated. The volume of the dispersion PFR was obtained by multiplying reactor total flow rate Q with hydraulic retention time (min) in the dispersion PFR, (L/u). Dead volume was determined by subtracting the CSTR working volume and dispersion PFR volume from total reactor volume. The last two parameters, D_p/L^2 and u/L were observed to vary with gas production rate. Dead volume and bypass

TABLE 2. Model Parameters Used in Simulation

Model parameters (1)	Value (2)
k_m[a] (gAc/gX-d)	5.11
K_s[a] (mM/L)	0.45
R[b] (mm)	1.5
ε[b]	0.69
δ[b] (μm)	100
Ar[b] (mm²)	1.05×10^6

Note: Simulated parameters are X_m (gVS/cm³), K_L (mm/s), f, V_b, D_p/L^2, u/L, and D (m²/s).
[a]Estimated from kinetic studies (Wu et al. 1995).
[b]Measured.

flow, $(1 - f)Q$, varied with operation and performance of the UASB reactor. Thus a converged range of these parameters were estimated.

RESULTS

Flow Modeling

Tracer study result is presented in Fig. 1(b). Recovery of lithium chloride was 100% at 5.3 HRT. The flow model describes the UASB reactor well. Estimated CSTR working volume, dispersion plug flow volume, dead volume, using the flow model, were 91, 2, and 7% of total volume, respectively (Table 3). Bypass flow occupied 24% of the total flow. This hydraulic model was further extended to account for substrate utilization and diffusion limitation during acetate perturbations.

Simulation of UASB Responses during Acetate Impulse Loading

During the acetate impulse experiment, acetate accumulated rapidly up to 10 mM and then decreased until below detection limits within 90 min. The dynamic model simulated acetate response curve is presented in Fig. 4. Under the experimental conditions, bypass flow was 14% of total flow. Dead volume, CSTR, and dispersion PFR occupied was 2, 96, and 2% of the reactor total volume, respectively. Gas production responded in a pattern similar to acetate (data not shown). A peak gas production value of 33 L/d was reached. This is five to six times that observed during normal operation (LiCl impulse, Table 1). Estimated model parameters were within a reasonable range. Diffusion coefficient of acetate within granules, D, was 33% of that in water (D_{water} = 13.3 × 10^{-10} m^2/s) (Bennett and Myers 1982). Reported literature values vary from 22–34% (Nilsson and Karlsson 1989; Speece 1988) and 40–80% (Alphenaar et al. 1993). A D of 34% of that in pure water has been used in a pH profile model and appeared adequate (Debeer et al. 1992). The mass transfer coefficient, K_L, was 0.013 mm/s, which is close to the reported value 0.009 mm/s (Inoue and Koyama 1989). A list of parameters estimated from the acetate impulse experiments are shown in Table 3.

Effects of hydraulic and diffusion-mass transfer on UASB reactor modeling were examined. A comparison was made among models involving hydraulics, reaction kinetics, or diffusion-mass transfer, including: (1) one CSTR with reaction-diffusion model; (2) two CSTR in series with reaction-diffusion model; (3) flow model [Fig. 1(a)] with reaction (no diffusion); and (4) the hydraulic-reaction-diffusion model. The computer program was modified for each of the preceding models during simulations. Results showed that the hydraulic (a nonideal CSTR coupled with a dispersion PFR)-reaction-diffusion model is the most satisfactory in describing the observed data (Figs. 5 and 6). Mass impulse to a CSTR is represented by a peak concentration at the beginning of the time course. Nonideal flow within the reactor produced a delay in the peak acetate concentration (Fig. 6). This delay is the HRT in the dispersion PFR. Neither a single CSTR nor two CSTR reactors in series adequately represent the UASB reactor (Fig. 6). The UASB reactor can't be adequately described without consideration of both hydraulic and diffusional factors. Hydraulics had the most pronounced effect (Fig. 6).

TABLE 3. Results Obtained from Acetate Impulse and Step Organic Loading Rate Increase and Lithium Chloride Impulse

Parameter (1)	LiCl impulse (2)	Acetate step increase (3)	Acetate impulse (4)
K_L (mm/s)	not applicable	0.013	0.013
D (m^2/s)	not applicable	4.42 × 10^{-10}	4.42 × 10^{-10}
f	0.76	0.99	0.86
D_p/L^2 (1/min)	0.001	0.0035	0.005
$V_{disp.PFR}$[b]	0.02V[a]	0.1V	0.02V
gas production rate (L/d)	5.3	1st step: 12.0 2nd step: 17.7	peak 33.6
V_b (CSTR working volume)	0.91V	0.90V	0.96V
V_d (dead volume)	0.07V	0V	0.02V

[a]V = reactor total volume.
[b]Calculated from u/L.

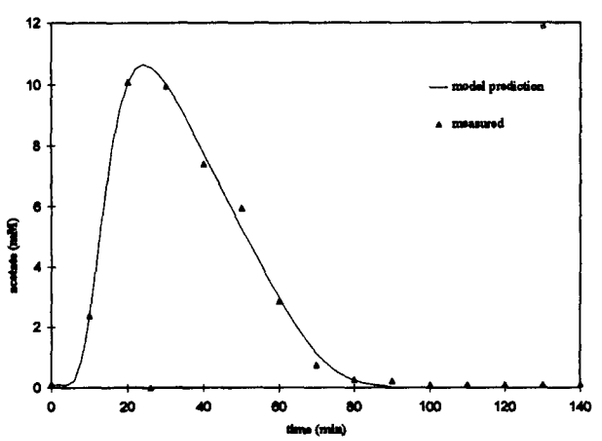

FIG. 4. Model Simulation of Acetate Concentration during Acetate Impulse and Measured Data from Bench-Scale UASB Reactor

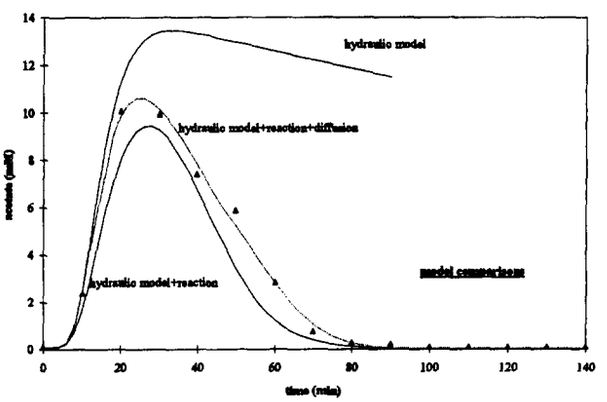

FIG. 5. Effect of Reaction and Diffusion in Modeling Data from Acetate Impulse Experiment

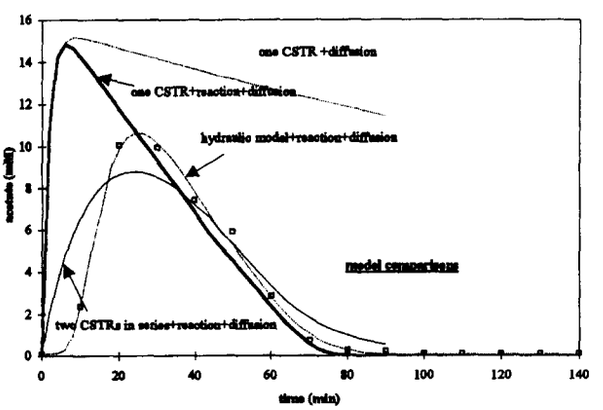

FIG. 6. Model Comparisons: One or Two CSTRs and Newly Developed Hydraulic Model with Reaction and Diffusion

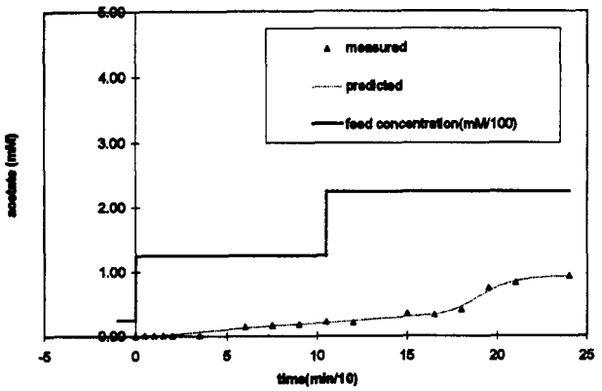

FIG. 7. Model Simulation Results of Effluent Acetate Concentration during Step Increase in Acetate Inlet Concentration Compared to Measured Data from Bench UASB Reactor

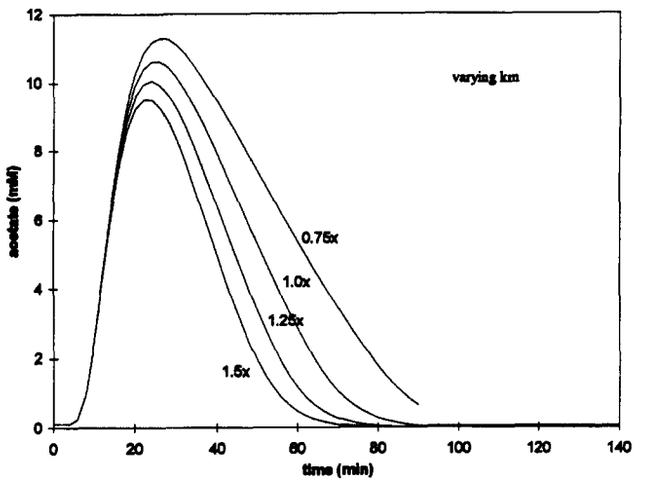

FIG. 8. Effect of Maximum Substrate Utilization Rate, k_m, on UASB Reactor Response during Acetate Impulse Experiment

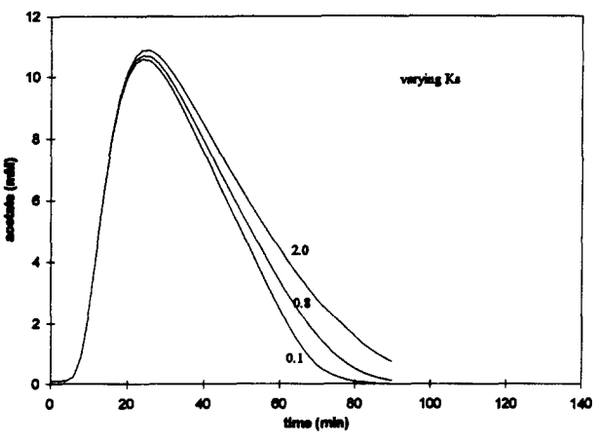

FIG. 9. Effect of Half Velocity Constant, K_s, on UASB Reactor Response during Acetate Impulse Experiment

Model Prediction during Acetate Step Increases

To verify the developed dynamic model, data obtained from the acetate loading rate step increase experiment was applied to the model and compared with the model prediction (Fig. 7). The observed responses of the UASB reactor to the acetate step increases were predicted by the model. Gas production rate increased, reaching 12 L/d for the first step and 17.7 L/d during the second step as a result of step input. Comparing results from acetate impulse and step increase, kinetic parameters (k_m, K_L), biomass parameters X_m, and mass transfer parameters D and K_L, remain consistent. The reactor working volume predicted by the model, were in a close agreement, 90–92% of the total reactor volume (Table 3). Dead volume and dispersion PFR volume were also within several percent. Two days prior to the experiment, the UASB reactor had a disturbance because the gas collector became clogged by granule clusters. The granule clusters were removed, consequently some granules were lost from the reactor. This incident affected the uniformity of the sludge bed and the bed volume, as observed in the reduction in dead volume from ~2–7% to 0, an increase in dispersion PFR volume from 2 to 10%, and only a small bypass flow of 1% of the total flow compared to 14–24% of the total flow from impulse experiments (Table 3). The increase in the PFR volume also resulted in a greater delay in system response (Fig. 7).

Sensitivity Analysis

Sensitivity analyses were performed on the model parameters k_m, K_s, D, R, K_L, V_d, and D_p/L^2 by simulation, where dead volume V_d is derived from V_b and V_{PFR}. Results were compared with the fitted value from acetate impulse experiment (Figs. 8–16). Responses of the UASB reactor appeared to be sensitive to the specific substrate utilization rate, k_m (Fig. 8). A large k_m tends to lower the response curve due to an increased biochemical reaction rate. The change in the response curves with respect to changes in k_m becomes more pronounced when k_m is small. A decrease in k_m of 25% has a much greater effect than an increase of the same magnitude (Fig. 8). The acetate

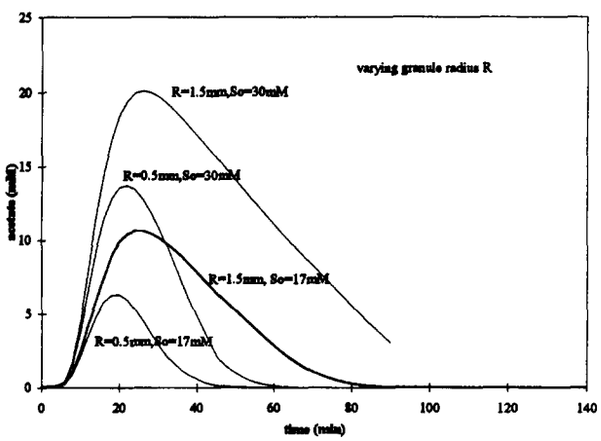

FIG. 10. Effect of Variation in Granule Radius R on UASB Response during Acetate Impulse at Different Initial Substrate Concentrations (S_o)

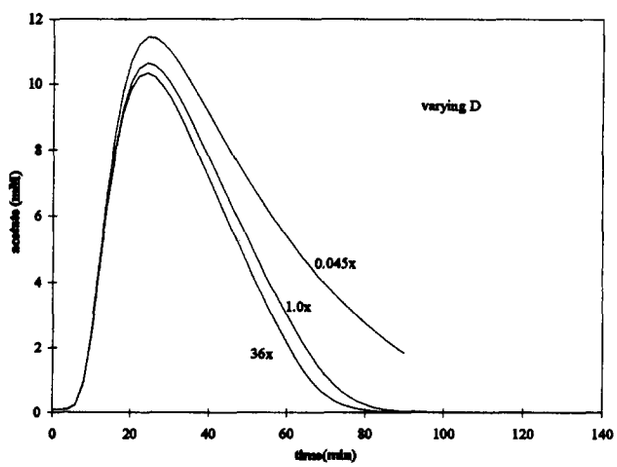

FIG. 11. Effect of Diffusion Coefficient, D, on Acetate Concentration Curve during Acetate Impulse

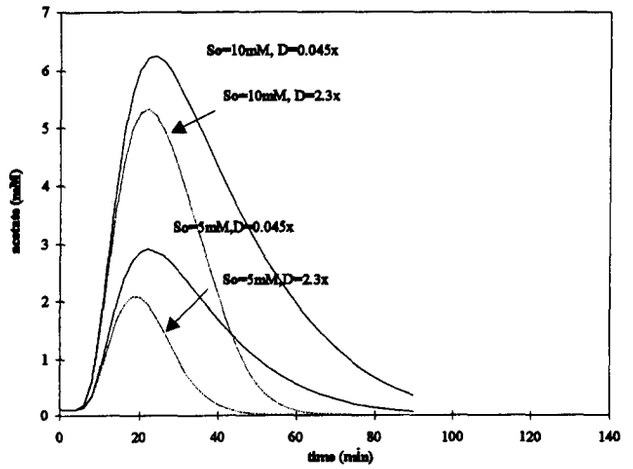

FIG. 12. Effect of Variations in Diffusion Coefficient, D, on UASB Response during Acetate Impulse at Different Initial Substrate Concentration (S_o)

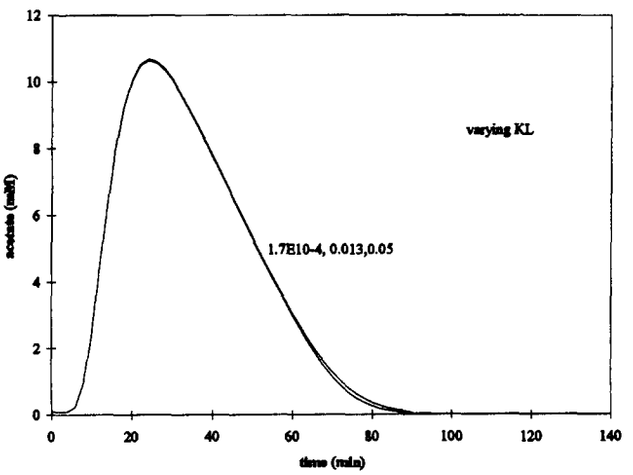

FIG. 13. Effect of Mass Transfer Coefficient, K_L, on UASB Response during Acetate Impulse

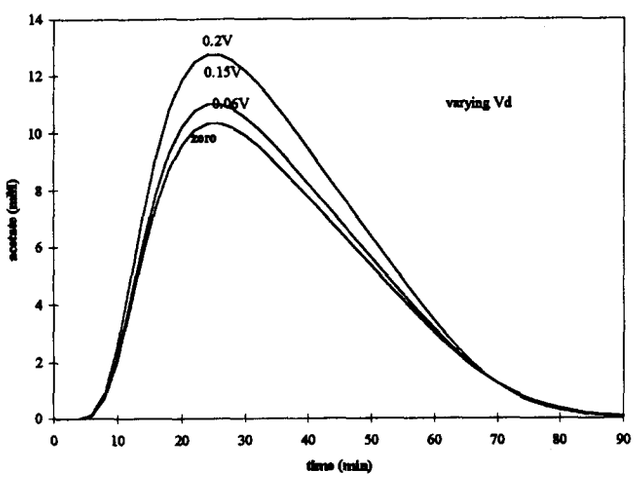

FIG. 14. Effect of Dead Volume, V_d, on Acetate Impulse Modeling

concentration curve decreases with a decrease in the half-velocity constant, K_s (Fig. 9). This is caused by an increased substrate affinity or greater slope in the Monod curve and subsequent increased reaction rate. The response curve is very sensitive to granule radius R (Fig. 10). When R is reduced by 1/3 (R = 0.5 mm from 1.5 mm), total surface area increases by a factor of 2.6 if the granule bed volume and the active biomass layer, δ, remain unchanged. As a result, mass flux rate into each granule is increased and overall substrate utilization rate increases; the concentration curve decreases. The effect of variation in the diffusion coefficient, D, on acetate utilization is shown in Figs. 11 and 12. Acetate concentration increases with a decrease in the diffusion coefficient suggests diffusional resistance. This change becomes small when the diffusion coefficient is large (i.e., 36 times; Fig. 10), which is an indication of improvement on mass transfer within granules. A change of same magnitude in the diffusion coefficient produces greater variation in the concentration curve at S_o = 5 mM than that at S_o = 10 mM (Fig. 12), suggesting that diffusion becomes less limiting when substrate flux is increased greatly. The mass transfer coefficient through liquid boundary layer, K_L, appears to have little effect (Fig. 13). Variations in K_L from 1.67×10^{-4} to 0.05 mm/s (300 times) did not result in any change in reactor acetate concentration, suggesting liquid film resistance was negligible in this system. Bulk acetate concentration increased with dead volume V_d (Fig. 14). Reactor total working volume was reduced as a result of the presence of dead volume. Therefore, the bulk acetate concentration increases. Reactor dispersion was analyzed using a dispersion factor D_p/L^2, as shown in (15). When the dispersion factor increased, the reactor effluent concentration decreased (Fig. 15). And, as expected, the response curve becomes wide and smooth, approaching the response of a completely mixed flow reactor. A decrease in the dispersion factor tends to increase the peak acetate concentration curve with

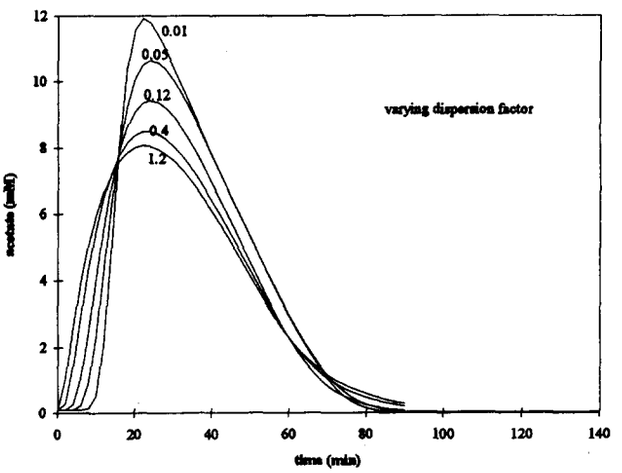

FIG. 15. Effect of Dispersion Factor, D_p/L^2 (×10), on UASB Response during Acetate Impulse

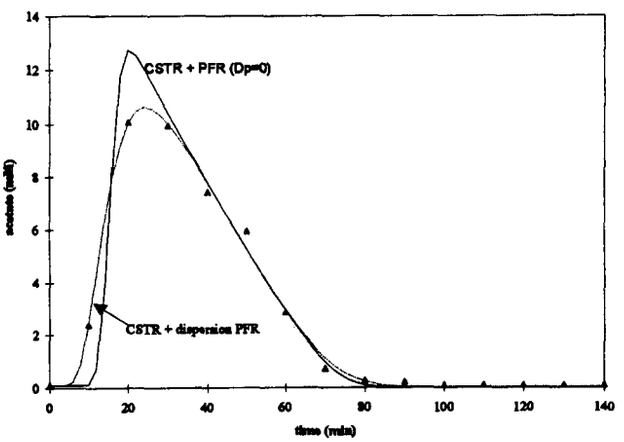

FIG. 16. Comparison of Dispersion PFR and PFR (Dispersion Factor is Zero) during Acetate Impulse Modeling

concurrent narrowing of the curve. In an extreme case, the dispersion factor equaling zero for the clarifier section, or, a CSTR + PFR model (Fig. 16), which obviously did not represent UASB reactor.

SUMMARY

Data from an acetate impulse experiment were simulated using the hydraulic-reaction-diffusion model with a good fit. Results from the acetate step increase experiments were predicted by the model using a single set of reaction and diffusion parameters. Results suggest that any of the three factors—kinetics; mass transfer and diffusion; and hydraulics—cannot be ignored in the dynamic model. Immediately after the introduction of an impulse, the distribution of acetate within the reactor is depended largely on reactor hydraulic (bypass, CSTR, PFR, etc.) and diffusional process. Kinetics (k_m, K_s) affects the second half of the response curve.

Results indicated that both reaction kinetics and diffusion contribute significantly in properly characterizing the performance of UASB reactors. Biochemical reaction kinetics (k_m and K_s) control system response to a large extent. However, there are great differences in the responses between dispersed cell systems (hydraulics-reaction model) and biofilm systems (hydraulic-reaction-diffusion model) (Fig. 5). These observations demonstrate the significant effect of diffusion. In granular sludge bed systems, when complete mixing is provided, the overall substrate utilization rate depends on coupled substrate transport and utilization kinetics. When the thickness of the granule outra (active) layer δ is constant, as observed in the brewery granules tested herein, and kinetic parameters (k_m, K_s) do not vary, the overall substrate utilization rate is sensitive to the granule radius R, and diffusion coefficient D. Granule radius appeared to be one of the most influential factors affecting substrate utilization in the UASB reactor (Fig. 10). Modeling results indicate a reduction in granule radius from 1.5 to 0.5 mm would result in a one-third reduction in the peak acetate concentration during acetate impulse (Fig. 10). Changes in K_L did not affect overall substrate utilization. This does not exclude the limitation of mass transfer within the liquid boundary layer because the thickness of this layer may have some effect. Results of the mass transfer experiment indicate a reduction of the liquid boundary layer could increase the overall acetate utilization rate (Wu et al. 1995).

Our study revealed significant influences of hydraulic behavior on reactor acetate concentration. One CSTR has often been assumed sufficient to describe UASB reactors. Results presented in Fig. 6 demonstrate that neither one CSTR with or without diffusion, nor two CSTRs in series with diffusion, could provide adequate description of the UASB reactor used in this work.

Reactor mixing was improved by an increase in biogas production. In this model, dispersion is a measure of substrate transport in the clarification zone in addition to advection. In the clarification zone, gas bubbles produced continuously migrate from the sludge bed; some granules pass upward through this volume when buoyed by attached gas bubbles. The dispersion factor, D_p/L^2, increases with applied OLR and, therefore, reactor gas production rate (Table 3). The gas production was maintained at the normal level in LiCl impulse experiment (5.3 L/d). An increase in the acetate concentration in feed by 100 mM resulted in gas production more than doubling in first step (12 L/d), and more than tripling for the second OLR step increase (17.7 L/d). An impulse of acetate resulted in 17 mM acetate in the reactor, produced a peak value of 33.6 L/d. The dispersion factor during these experiments increased from 0.001 to 0.005 for the LiCl impulse and acetate impulse experiments, respectively (Table 3).

CONCLUSIONS

UASB reactor performances under acetate impulse and step increases can be described by a dynamic hydraulic-reaction-diffusion model. A CSTR with dead volume and bypass flow, followed by a dispersion PFR represents well the flow of the bench-scale UASB reactor used in this experiment. Each term in the dynamic model: hydraulics, degradation kinetics, and diffusion process, plays an important role. The response of UASB reactors is most sensitive to variations in granule radius R and least sensitive to the liquid film mass transfer coefficient K_L. In general, hydraulic parameters have a pronounced influence on the reactor performance.

ACKNOWLEDGMENTS

The writers wish to acknowledge the New York State Energy Research and Development Authority, in particular Barry Liebowitz, who supplied funds for this work, under the contract No. 1738-ERER-MSW-92 to the Michigan Biotechnology Institute.

APPENDIX I. REFERENCES

Alphenaar, P. A., Perez, M. C., and Lettinga, G. (1993). "The influence of substrate transport limitation on porosity and methanogenic activity of anaerobic sludge granules." *Appl. Microbiol. Biotechnol.*, 39, 276–280.

Ames, W. F. (1977). *Numerical methods for partial differential equations.* W. Rheinboldt, ed., Academic Press, Inc., San Diego, Calif.

Andrews, J. F. (1969). "A mathematical model for the continuous culture of microorganisms utilizing inhibitory substrate." *Biotechnol. Bioengrg.*, 10, 707–723.

Andrews, G. (1988). "Fluidized-bed bioreactors." *Biotechnol. and Genetic Engrg. Rev.*, 6, 151–178.

Andrews, J. F., and Graef, S. P. (1971). "Dynamic modeling and simulation of the anaerobic digestion process." *Anaerobic biological treatment process*, Vol. 105, Am. Chemical Soc., Washington, D.C., 126–162.

Atkinson, B., and Davies, I. J. (1974). "The overall rate of substrate uptake (reaction) by microbial films. Part I. A biological rate equation." *Trans. Inst. Chemical Engrs.*, 52, 248–259.

Atkinson, B., and Daoud, I. (1970). "Diffusion effects within microbial films." *Trans. Inst. Chemical Engrs.*, 48, T245–T254.

Atkinson, B., and How, S. Y. (1974). "The overall rate of substrate uptake (reaction) by microbial films." *Trans. Inst. Chemical Engrs.*, 52, 260–268.

Benefield, L., and Molz, F. (1984). "A model for the activated sludge process which considers wastewater characteristics, floc behavior and microbial population." *Biotechnol. Bioengrg.*, 26, 352–361.

Bennett, C. O., and Myers, J. E. (1982). *Momentum, heat and mass transfer*, 3rd Ed., McGraw-Hill Book Co., Inc., New York, N.Y.

Bolle, W. L., van Breugel, J., van Eybergen, G. C., Kossen, N. W. F., and van Gils, W. (1985). "An integral dynamic model for the UASB reactor." *Biotechnol. Bioengrg.*, 28, 1621–1636.

Bolte, J. P., and Hill, D. T. (1993). "A comprehensive dynamic model of attached growth anaerobic fermenters." *Trans. ASAE*, 36(6), 1805–1814.

Buffière, P., and Steyer, J. P. (1995). "Comprehensive modeling of methanogenic biofilms in fluidized bed systems: mass transfer limitations and multisubstrate aspects." *Biotechnol. Bioengrg.*, 48, 725–736.

Carr, A. D., and O'Donnell, R. C. (1977). "The dynamic behavior of an anaerobic digestor." *Progress in Water Technol.*, 9, 727–738.

De Beer, D., Huisman, J. W., Van den Heuvel, J. C., and Ottengraf, S. P. P. (1992). "The effect of pH profiles in methanogenic aggregates on the kinetics of acetate conversion." *Water Res.*, 26(10), 1329–1336.

Harremoës, P. (1976). "The significance of pore diffusion to filter denitrification." *J. Water Pollution Control Fedn.*, 48(2), 377–388.

Hill, D. T., and Barth, C. L. (1977). "A dynamic model for simulation of animal waste digestion." *J. Water Pollution Control Fedn.*, 10, 2129–2143.

Inoue, Y., and Koyama, K. (1988). "Mechanism of volatile fatty acid removal in a fixed biofilm methane fermentation reactor." *Water Sci. Technol.*, 20(11), 377–383.

Kissel, J. C., McCarty, P. L., and Street, R. L. (1984). "Numerical simulation of mixed culture biofilm." *J. Envir. Engrg.*, ASCE, 110(2), 393–411.

LaMotta, E. J. (1976). "Internal diffusion and reaction in biological films." *Envir. Sci. Technol.*, 10(8), 765–774.

Lens, P. N. L., De Beer, D., Cronenberg, C. C. H., Houwen, F. P., Ottengraf, S. P. P., and Verstraete, W. H. (1993). "Heterogeneous distribution of microbial activity in methanogenic aggregates: pH and glucose microprofiles." *Appl. Envir. Microbiol.*, 59(11), 3803–3815.
Lin, S. H. (1991). "A mathematical model for a biological fluidized bed reactor." *Chemical Tech. Biotechnol.*, 51, 473–482.
Mosey, F. E. (1983). "Mathematical modeling of the anaerobic digestion process: regulatory mechanisms for the formation of short-chain volatile acids from glucose." *Water Sci. Technol.*, 15(8), 209–219.
Nilsson, B. K., and Karlsson, H. T. (1989). "Diffusion rates in a dense matrix of methane-producing microorganisms." *J. Chemical and Tech. Biotechnol.*, 44, 255–260.
Rittmann, B. E. (1982). "The effect of shear stress on biofilm loss rate." *Biotechnol. Bioengrg.*, 24, 501–506.
Rittmann, B. E., and McCarty, P. L. (1980). "Model of steady-state-biofilm kinetics." *Biotechnol. Bioengrg.*, 22, 2343–2357.
Rozzi, A. S., Merlinio, S., and Passino, R. (1985). "Development of a four population model of the anaerobic degradation of carbohydrates." *Envir. Technol. Letters*, 6, 610–619.
Shieh, W., Mulcahy, L. T., and LaMotta, E. J. (1982). "Mathematical model for the fluidized bed biofilm reactor." *Enzyme Microbiol. Technol.*, 4(Jul.), 269–276.
Speece, R. E. (1988). "A survey of municipal anaerobic sludge digestors and diagnostic activity assays." *Water Res.*, 22, 365–372.
Wu, M. M. (1995). Characterization of performance and monitoring of the Upflow Anaerobic Sludge Blanket Reactor," PhD thesis, Michigan State Univ., East Lansing, Mich.
Wu, M. M., Criddle, C. S., and Hickey, R. F. (1995). "Mass transfer and temperature effects on substrate utilization in brewery granules." *Biotechnol. Bioengrg.*, 45, 465–475.

APPENDIX II. NOTATION

The following symbols are used in this paper:

A_r = total granule surface area (mm^2);
D = effective substrate diffusion coefficient (m^2/s);
D_p = dispersion coefficient of liquid in PFR (mm^2/s);
D_p/L^2 = dispersion factor for clarifier (l/s);
$E(t)$ = input function;
f = fraction;
K_l = mass transfer coefficient (mm/s);
K_s = half velocity constant (mM);
k_m = specific substrate utilization rate (g acetate/gVS-d);
L = length of PFR;
Mf = mass input that enters reactor working volume (g);
Qf = flow that enters main stream (L/d);
R = granule radius (mm);
S = substrate concentration within granules at unsteady state (mM);
S_b = bulk substrate concentration (mM);
S_d = concentration in clarification zone (mM);
S_s = substrate concentration within biofilm at steady state (mM);
S_{bo} = steady-state substrate concentration in bulk liquid (mM);
S_{bkgd} = influent substrate concentration before step increase (mM);
S_{stp1} = influent substrate concentration at first step increase (mM);
S_{stp2} = influent substrate concentration during second step increase (mM);
T_{in} = substrate injection time for acetate impulse (min);
T_{stp1} = time that first step is initiated (min);
T_{stp2} = time that second step is initiated (min);
u = flow velocity in PFR (mm/s);
u/L = inverse HRT within dispersion PFR (min);
V_b = working volume of CSTR (L);
V_d = dead volume (L);
V_t = reactor total liquid volume (L);
x = axis originating from surface of granules toward central core; and
X_m = active acetate utilizer biomass density within granules (gVS/cm^3).